Influence of acrylamide on ROS, Hsp27 and NF-κB in bone marrow mesenchymal stem cells

YANG LIU[1], XIAOLI TAO [2], YULIAN MU[3], PAN WANG[4], SHUTANG FENG[5] and KUI LI[6]

Institute of Animal Sciences, Chinese Academy of Agricultural Sciences, Beijing 100193 China

ABSTRACT

The bone marrow mesenchymal stem cells (BM-MSCs) treated with acrylamide (ACR) were used to make out the immune response to ROS, interleukin-8 and phosphorylated Hsp27 of ACR. ACR was reported as a probable human carcinogen, neurotoxic and mutagenic. BMMSCs have the capability of immunoregulation, and participate in the process of multiple immune response. It has attracted the attention of researchers that these cells have priority to move to the damaged tissue, as a kind of potential therapeutic tool for tissue repair. ACR and BMMSCs are related to immune reactions, especially those involving in tumours and cancers. However, the interaction between ACR and BMMSCs is still poorly understood. In present study, we report the influence of ACR on BMMSCs. At first, BMMSCs were disposed with 0.5mM ACR for 72 h, and then the secretion of ROS, interleukin-8, phospho-Hsp27 and NF-κB activities, apoptosis and cell cycle, respectively, were determined. The results showed that the secretion of ROS, interleukin-8 and phosph-Hsp27 increased and NF-κB was activated, while the apoptosis and cell cycle have no obvious alteration. In conclusion, ACR probably activated the NF-κB pathway in BMMSCs via oxidative stress, which may provide new insights to study the immune response and the influence mechanism of ACR.

Key words: Acrylamide, Bone marrow mesenchymal stromal cells, Hsp27, NF-κB, Porcine, ROS

As a small hydrophilic molecule, acrylamide (ACR) has wide applications in the polymer industry, and individuals can be exposed to ACR in their workplace or in the environment (Fennell *et al.* 2015). Since 2002, researchers have determined that foods cooked at high temperatures, especially several heated carbohydrate-rich foods such as potato chips and French fries, contain relatively high acrylamide levels (Konings *et al.* 2007). Ingestion of these foods may noticeably increase the risk of human exposure to ACR (Pelucchi *et al.* 2015). Some reports have demonstrated that ACR is a probable human carcinogen and displays clastogenic, neurotoxic (Pennisi *et al.* 2013) and mutagenic properties in somatic and germ cells in animal models. In theory, all of the tissues may become targets for ACR-mediated carcinogenesis because the ACR molecule is small and hydrophilic, and passively diffuses throughout the entire body. Previously, epidemiologic

studies on the effects of ACR demonstrated positive correlations with the risk of ovarian, endometrial and renal cell cancers (Hogervorst *et al.* 2007, 2008).

MSCs have eximious potential for repairing tissue damage that is caused by immune responses. Previous studies have suggested that intravenously infused MSCs immigrate to inflammatory or injured tissues (Tanaka 2015). MSCs possess the capability to inhibit or modulate immune responses *in vivo* (Abdi *et al.* 2008). The bone marrow mesenchymal stem cells (BMMSCs), as one type of MSCs, also possess the aforementioned characteristics, may be used as a potential therapeutic tool for tissue repair, which has attracted the attention of researchers (Keating 2006, Chamberlain *et al.* 2007). Although MSC infusion is considered to be relatively safe, recent studies have suggested that MSCs may become neoplastic after long-term culture and, following infusion can enhance tumour growth in some, but not all experimental models. Additionally, the analysis of a H1 ESC-derived MSCs has shown that these cells produce a factor (or factors) that robustly induces NF-κB activity in multiple myeloma (MM) cells in a bortezomib-resistant manner (Markovina *et al.* 2010). These ESC-derived MSCs express cell surface markers and possess multilineage differentiation potentials that are similar to normal bone marrow MSCs (Trivedi *et al.* 2008, Markovina *et al.* 2010). Another group has shown

Present address: [1](ml417530@126.com), [4,5,6](1033904909 @qq.com, fst508@sina.com, kuili@iascaas.net.cn), [3]Principal Scientist (muyulian76@iascaas.net.cn), State Key Laboratory of Animal Nutrition and Key Laboratory of Farm Animal Genetic Resources and Germplasm Innovation of Ministry of Agriculture. [2](taoxiaoli521@sina.com), Chinese Academy of Agricultural Sciences and College of Animal Husbandry and Veterinary, Liaoning Medical University.

that TNF-α dramatically increases human MSC (HMSC) migration via extracellular matrix interactions, which is partially regulated by the NF-κB pathway (Bocker *et al.* 2008).

Nuclear factor-kappa B (NF-κB) belongs to a family of inducible transcription factors (Dos Santos Nascimento *et al.* 2015), which involve cytokine- or pathogen-induced upregulation of inflammatory cytokines and subsequent immune responses. However, under certain circumstances, inflammatory cytokines may become immunosuppressive. For example, bone marrow stromal cells (BMSCs) from MM patients uniquely enhance the constitutive NF-κB activity in MM cells via a proteinaceous secreted factor in conjunction with interleukin-8 (IL-8) (Markovina *et al.* 2010).

In a word, we demonstrated that ACR activated the NF-κB pathway in BMMSCs. It lays a foundation for further studies of the influence mechanism of ACR. At the same time, it also provides experimental and theoretical basis for better applicating MSCs in the clinical treatment.

MATERIALS AND METHODS

Isolation and culture of porcine MSCs: Femur and tibia bones from 6-day to 6-month-old porcine (n>3) were isolated to extract the gelatinous bone marrow under sterile conditions, and had been evaluated by flowcytometric analysis, adipogenic and osteogenic differentiation as described previously (Huang *et al.* 2015). The extracted gelatinous bone marrow was resuspended in DMEM/F-12 (Dulbecco's Modified Eagle Medium, Nutrient Mixture F-12) and dispersed gently. Samples were centrifuged (1,000 rpm, 5 min) and resuspended in 5 ml of DMEM/F-12 containing 15% fetal bovine serum (FBS) and 1% pen/strep. The cells were seeded in a 100-mm culture plate at a concentration of $1 \times 10^6/cm^2$ and incubated in a humidifled 5% CO_2 atmosphere at 37°C. Nonadherent cells were gently rinsed off by replacing half of the culture medium after plating cells for 48 h. The attached MSCs were confluent after 5–7 days (passage 0). For every passage, cells were trypsinised using a 0.25% Trypsin-EDTA solution. With the exception of passage 0, the FBS content in the complete culture medium was changed to 10% FBS. Thereafter, the culture medium was changed every 3 days to promote cell growth. The cells were split approximately 1:2 at each passage after the culture reached 80–90% confluency.

Measurement of reactive oxygen species: The content of the reactive oxygen species (ROS) that were produced by BMMSCs treated with ACR was determined using the ROS Assay Kit. Cells were seeded in a 96-well cell culture plate at a concentration of 3×10^4 cells/well in D-MEM/F-12, containing 10% FBS, 1% pen/strep and cultured at 37°C in a humidifled atmosphere with 5% CO_2 for 12 h. The medium was changed before treating the cells with 0.5 mM (the optimal one according to the concentration gradient filter) ACR for 72 h. At the end of the treatment period, the medium in each well was removed, cells were washed with PBS, and the DCF of ROS assay was performed according to the kit instructions. The fluorescence was measured using a microplate fluorescence reader using a 488 nm excitation wavelength with a 525 nm emission fllter.

Measurement of phosphorylated Hsp27 by ELISA: Phospho-Hsp27 in control and ACR-treated BMMSCs was measured using ELISA. BMMSCs were seeded in 96-well plates at a concentration of 2×10^4 cells/well and treated with 0.5 mM ACR. Control cells were treated with complete culture medium. After 72 h, cells from the 2 groups were collected and prepared for the detection of phospho-Hsp27 according to the manufacturer's protocol. The plate was read using a fluorescence plate reader with an excitation wavelength at 540 nm and an emission wavelength at 600 nm, followed by an excitation wavelength at 360 nm and an emission wavelength at 450 nm. The readings at 600 nm represented the amount of phosphorylated Hsp27 in the cells, and the readings at 450 nm represented the amount of total cytochrome c in the cells.

Measurement of IL-8 secretion by ELISA: Secretion of IL-8 in the spent media of control and ACR-treated BMMSCs was measured with the Quantikin® Porcine IL-8/CXCL8 Immunoassay. Cells were treated with ACR as described above for 72 h. The supernatants of the ACR-treated cells and control cells were collected according to the manufacturer's protocol. The optical density was read using a fluorescence plate reader with the emission wavelength set to 450 nm and the correction wavelength at 540 nm. IL-8 concentrations of the 2 groups were extrapolated from a standard curve that was derived using known concentrations of IL-8. Sample values were normalised to the total cell protein concentrations, which were determined using the BCA protein assay.

Relative quantiflcation of IL-8 gene expression by real-time PCR: Total RNA of BMMSCs cultured for 72 h in culture medium containing 0.5 mM ACR were extracted. One microgram of total RNA was reverse-transcribed into cDNA with oligo (dT) primers. For real-time PCR, the following primers were designed using the Primer 5.0 software IL-8 F: 5'-tctatgcctcattcctgtgc-3', IL-8 R: 5'-atagaacaacgtgcatggga-3'. GAPDH F: 5'-ggtgaaggtcggagtgaacg-3', GAPDH R: 5'-ctcgctcctggaagatggtg-3'.

Real-time PCR was performed using the ABI 7500 real-time PCR system with the Real Master Mix (SYBR Green). The RT-PCR conditions were as follows: 50°C for 2 min and denaturation at 95°C for 30 sec followed by 40 cycles of denaturation at 95°C for 20 sec, reannealing at 60°C for 30 sec, and extension at 72°C for 30 sec. The gene GAPDH was used as an internal control to normalise cDNA quantity. The expression level of target gene was quantified using the comparative threshold (Ct) method. Each real-time PCR reaction was performed in triplicate, and the data were shown as mean ± SE (n=3). The significant differences were determined using the one-way analysis of variance (ANOVA) test using SPSS software 13.0, and the significance levels were set to P<0.05.

Transfection, luciferase reporter assays: BMMSCs were seeded in 96-well plates at a density of 2×10^4 cells/well. Once cells reached approximately 60% confluence, the cells were transfected using Lipofectamine 2000 using a procedure of Li *et al.* (2011).The samples were divided into 3 groups, as follows: positive, ACR-treated and control groups. Samples were transfected with 70 ng/well of the reporter plasmid pNF-κB-Lucand 70 ng/well of pRL-TK plasmid for the control and ACR-treated groups, 70 ng/well of the expression plasmid pcDNA3.1(+)-pp65 (Li *et al.* 2011) to induce pp65 overexpression as the positive control or 70 ng/well of the empty control plasmid pcDNA3.1(+) as the negative. After 6 h of the transfection, the culture medium of the treatment group was replaced with complete culture medium containing 0.5 mM ACR. The media of the other groups were placed with normal culture media. Luciferase assays were performed 72 h after transfection using the dual-speciflc luciferase assay kit according to the manufacturer's directions. All of the reporter assays were repeated at least three times. The samples were collected according to the manufacturer's protocol.

Cell cycle analysis: Cells (Passage 3–6) were harvested using 0.25% trypsin, washed in PBS and flxed in absolute ethanol at –20°C. The cells were washed once with PBS, incubated with DNA staining solution containing propidium iodide and RNase A for 30 min at room temperature and analysed using FACS Calibur flow cytometry.

Analysis of cell apoptosis: Apoptotic cells (Passage 3–6) were detected using the Annexin V-FITC apoptosis detection kit using the manufacturer's protocol. Cells were collected after ACR treatment and resuspended in PBS. Approximately 1×10^6 cells were incubated with Annexin V-FITC and analysed using FACS Calibur flow cytometry.

Statistical analysis: Data were expressed as mean ± SE. The statistical significance was determined in all of the experiments using the one-way ANOVA test by SPSS software 13.0. Student's t-test was also used to evaluate the statistical significance. $P < 0.05$ were considered statistically significant.

RESULTS AND DISCUSSION

ACR-induced increase in ROS: After ACR treatment (0.5 mM) for 72 h, the DCF of ROS in the BMMSCs markedly rose compared to that of the control group (Fig. 1). It illustrated that the ROS production increased. The differences between ACR-treated and control cells were statistically significant ($P < 0.01$).

Under normal conditions, the system of ROS generation and scavenging is maintained in a dynamic equilibrium *in vivo*. Previous studies showed that oxidative stress is involved in chromosomal aberrations, gene mutations, tumour formation and cancer development. ROS provides a mechanism for significant indirect genotoxicity (Vinoth *et al.* 2015). The above results indicated that ACR treatment increased the production of ROS in cells, creating an oxidative-stressed state. Under these conditions, ROS generation may occur at a relatively higher rate than ROS

scavenging. Imai *et al.* 2008 showed that viral infection caused oxidative stress. In addition, previous studies have suggested that lipopolysaccharide (LPS) and dextran sodium sulphate (DSS) increase ROS production and regulate the subsequent activation of the NF-κB pathway in colonic epithelial cells (Bhattacharyya *et al.* 2008, 2009). A similar mechanism may exist among these xenobiotics to increase the ROS generation. Increasing ROS generation may decrease the secretion of Hsp27 and promote the activation of the NF-κB pathway and apoptosis in epithelial cells (Bhattacharyya *et al.* 2008). Therefore, we further examined the influence of ACR on Hsp27 and NF-κB activity in BMMSCs.
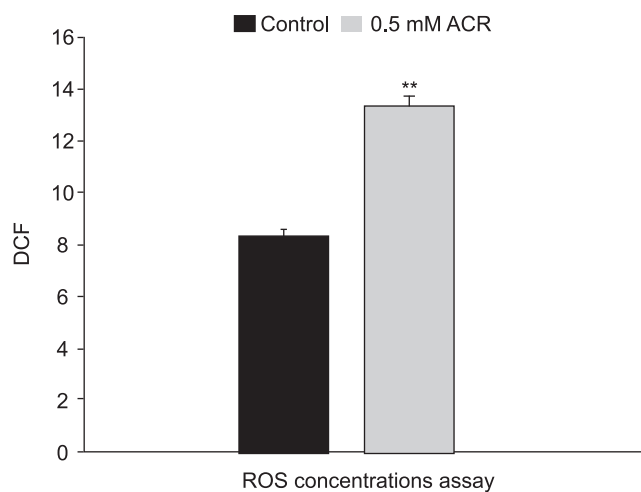

Fig.1. Increased reactive oxygen species (ROS) producion following ACR exposure in BMMSCs. BMMSCs in culture was treated with ACR (0.5mM) for 72 h and the DCF of ROS was measured. Differences between the control and treated cells are statistically significant ($P < 0.05$). Control group was BMMSCs cultured in normal medium.

ACR-induced increase in phospho-Hsp27 secretion from BMMSCs: Phospho-Hsp27 was assayed using cell-based ELISA in control and ACR-treated BMMSCs. Compared with control group, phospho-Hsp27 was dramatically increased ($P < 0.05$) following ACR treatment for 72 h (Fig. 2).

The heat shock response produces HSP under negative conditions and is highly conserved among different species. In normal cells, the expression of Hsp27 is low. However, when cells are exposed to heat stress, oxidative stress or other stressful stimuli, Hsp27 expression rapidly increases. Under high-concentrations of ACR (10–20 mM), cell viability significantly decreases (Cao *et al.* 2008). The above results manifested that the cells were treated with low-concentration ACR (0.5 mM), and Hsp27 levels increased compared to that of the control group. Therefore, we concluded that a low concentration of ACR-treatment was sufficient to increase Hsp27 expression.

ACR caused activation of NF-κB in BMMSCs: To examine the transactivational ability of ACR, the mammalian expression vector harbouring the coding
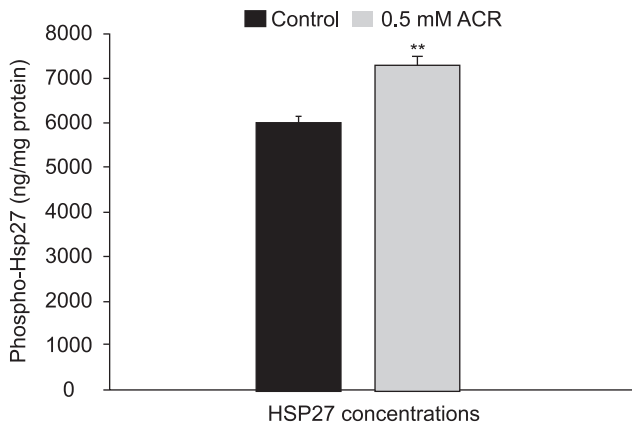
Fig. 2. Phospho-Hsp27 was detected after BMMSCs treated with ACR (0.5mM) for 72 h. Compared with control group, the Phospho-Hsp27 production increased remarkably (P<0.05).

sequence of pp65 [pcDNA3.1(+)-pp65] and the luciferase reporter gene vectors were cotransfected into the ACR-treated and control BMMSCs. ACR remarkably increased (P<0.01) the luciferase activity (Fig. 3) of the reporter gene vector (pNF-κB -Luc).

The results showed that the NF-κB pathway was activated after BMMSCs were treated with ACR. Previous researchers have implied that NFκB transcription factors play a key role in the survival and proliferation of B-cell tumours, including multiple myeloma (MM) cells (Markovina *et al.* 2010, Demchenko *et al.* 2010). In MM, the activation of NF-κB in BMMSCs may uniquely promote NF-κB activity in MM cells but not normal cells. Djouad *et al.* (2003) reported that the subcutaneous injection of B16 melanoma cells induces tumour growth in allogeneic recipients only with the co-injection of MSCs (Abdi *et al.* 2008). Whether ACR-induced NF-κB activation in BMMSCs participates in the process of carcinogenesis requires further investigation.
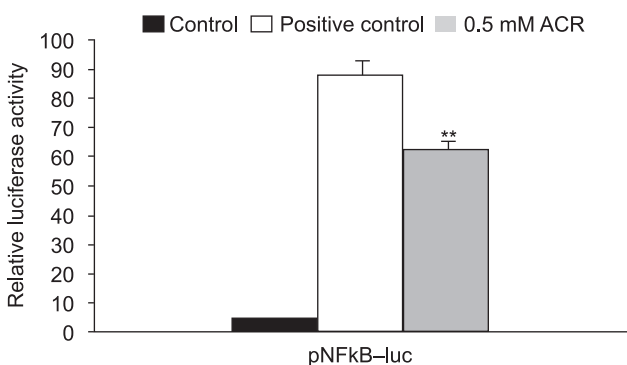
ACR-induced increase in IL-8 secretion from BMMSCs:

Fig. 3. Dual luciferase assay with reporter vector pNF-κB-luc in BMMSCs. The luciferase activities were both significantly increased in BMMSCs which were induced by 0.5mM ACR and positive control which was transfected by overexpression of pp65 (P < 0.05). All luciferase assays were repeated at least three times and data shown represent the mean±SE (n = 3) from one representative experiment.
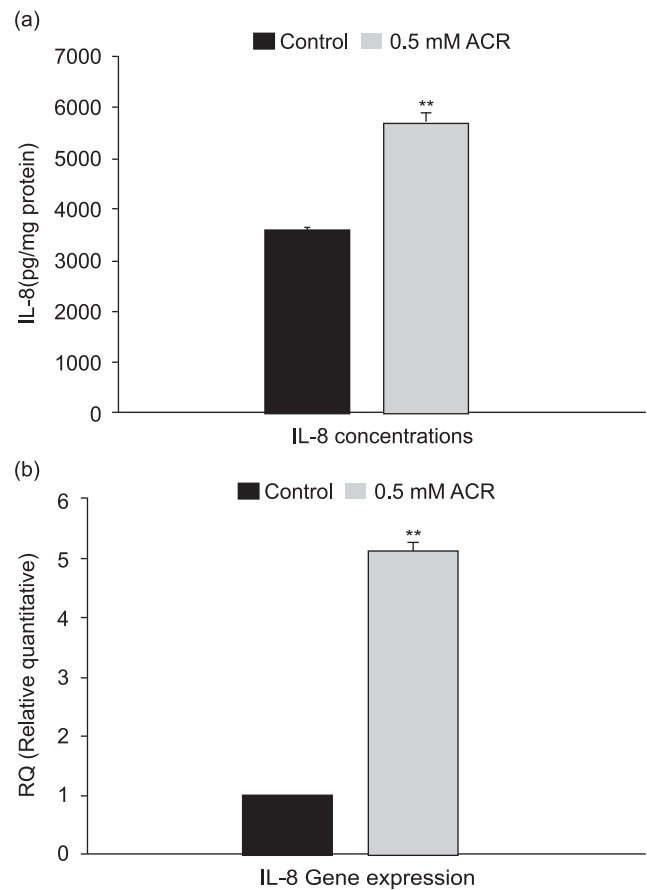
(a)

(b)

Fig. 4 (a) IL-8 secretion was detected after ACR induced for 72 h. IL-8 secretion from BMMSCs was descreased when cells were treated with ACR (0.5mM) for 72 h. ACR increased IL-8 secretion obviously compared with control (P<0.05). (b) Expression of IL-8 in ACR(0.5mM) treated BMMSCs and control assessed by real-time PCR. Error bars indicate the SE (n = 3) of relative mRNA expression levels of IL-8 to GAPDH, determined by real-time quantitative PCR. Compare with control group, gene expression of IL-8 was increased significantly (P < 0.05). The experiments were repeated three times.

IL-8 was assayed using ELISA assay kit in control and ACR-treated BMMSCs. After 0.5mM ACR treated for 72h, the level of IL-8 secretion from the BMMSCs increased obviously compared with control group (P<0.05) (Fig. 4a). In addition, we analysed the mRNA expression of IL-8 in ACR-treated and control BMMSCs. Real-time PCR analysis revealed that the mRNA expression profiles of IL-8 in ACR-treated BMMSCs was significantly increased (P<0.05) compared to those in control BMMSCs (Fig. 4b). The activation of NF-κB in BMMSCs upregulates inflammatory factors such as IL-8. IL-8 contributes to BMSC-induced NF-κB activity in MM cells (Markovina *et al.* 2010). The above results demonstrated that the expression of NF-κB pathway downstream inflammatory factor IL-8, increased at the mRNA and protein levels.

Cell cycle and apoptosis: The cell cycle was examined using a cell cycle stainingsolution by flow cytometry. As shown in Fig. 5, no obvious differences were observed between ACR-treated and control BMMSCs. The apoptosis

was measured using annexin V and the dead cell apoptosis kit after ACR treatment for 72 h. The fluctuation of apoptotic rates was not observed after ACR treatment (Fig. 6).

The anti-oxidation stress activities of Hsp27 play a remarkably role in anti-apoptosis and may promote the proliferation of BMMSCs. Conversely, cells that were treated with high concentrations of ACR might decreased Hsp27 expression, which promoted ROS generation and activation of the NF-κB pathway to induce apoptosis. However, the apoptosis-promoting function of Hsp27 was generally restricted because the protective effect of HSP was predominant. This microregulated balance is the key to cell death or survival and functions as the transition centre between cell necrosis and apoptosis.

In conclusion, ACR is gaining more notoriety as a common compound in our daily life. The current report studied the immune reaction of ACR-treated BMMSCs. We hypothesised that BMMSCs stimulated with 0.5 mM ACR displayed and increase in the secretion of ROS, phospho-Hsp27 and IL-8 and the activation of NF-κB as well as no

obvious changes in apoptosis and proliferation. Further investigation is required to detect the influence of high concentrations of ACR on BMMSCs. The conclusions of the current study may help elucidate the mechanism of ACR on immune responses.

ACKNOWLEDGEMENT

REFERENCES

Abdi R, Fiorina P, Adra C N, Atkinson M and Sayegh M H. 2008. Immunomodulation by mesenchymal stem cells: a potential therapeutic strategy for type 1 diabetes. *Diabetes* **57**: 1759–67.

Bhattacharyya S, Dudeja P K and Tobacman J K. 2008. Lipopolysaccharide activates NF-kappaB by TLR4-Bcl10-dependent and independent pathways in colonic epithelial cells. *American Journal of Physiology-Gastrointestinal and Liver Physiology* **295**: G784–90.

Bhattacharyya S, Dudeja P K and Tobacman J K. 2009. ROS, Hsp27, and IKKbeta mediate dextran sodium sulfate (DSS) activation of IkappaBa, NFkappaB, and IL-8. *Inflammatory Bowel Diseases* **15**: 673–83.

Bocker W, Docheva D, Prall W C, Egea V, Pappou E, Rossmann O, Popov C, Mutschler W, Ries C and Schieker M. 2008. IKK-2 is required for TNF-alpha-induced invasion and proliferation of human mesenchymal stem cells. *Journal of Molecular Medicine* **86**: 1183–92.

Cao J, Liu Y, Jia L, Jiang L P, Geng C Y, Yao X F, Kong Y, Jiang B N and Zhong L F. 2008. Curcumin attenuates acrylamide-induced cytotoxicity and genotoxicity in HepG2 cells by ROS scavenging. *Journal of Agricultural and Food Chemistry* **56**: 12059–63.

Chamberlain G, Fox J, Ashton B and Middleton J. 2007. Concise review: mesenchymal stem cells: their phenotype, differentiation capacity, immunological features, and potential for homing. *Stem Cells* **25**: 2739–49.

Demchenko Y N and Kuehl W M. 2010. A critical role for the NFkB pathway in multiple myeloma. *Oncotarget* **1**: 59–68.

Djouad F, Plence P, Bony C, Tropec P, Apparailly F, Sany J, Noee D and Jorgensen C. 2003. Immunoruppressive effect of merenchymal stem cell, favours tumour growth in allogenlic animals. *Blood* **102**: 3837–44.

Dos Santos Nascimento M V, Arruda-Silva F, Luz A B, Venzke D, Queiroz G S, Mendes B G, Fernandes-Ribeiro E R, Frode T S, Pizzolatti M G and Dalmarco E M. 2015. 7-prenyloxi–6-methoxycoumarin from Polygala sabulosa A.W. Bennett Regulates p38 MAPK and NF-kB Pathways Inhibiting the Inflammation Induced by Carrageenan in the Mouse Model of Pleurisy. *Inflammation and Allergy Drug Targets* 14 (1): 37–46.

Fennell T R, Snyder R, Hansen B and Friedman M. 2015. Dosimetry of Acrylamide and Glycidamide Over the Lifespan in a 2–Year Bioassay of Acrylamide in Wistar Han Rats. *Toxicological Sciences* **146**: 386–94.
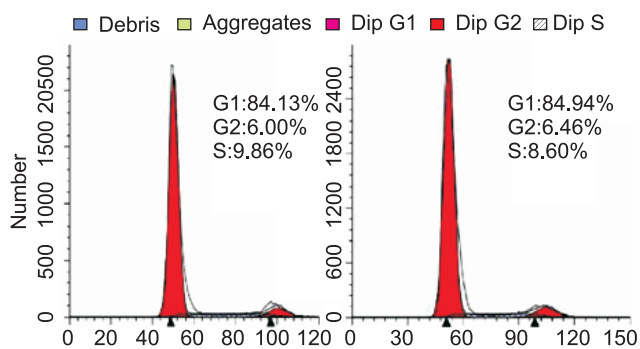

Fig. 5. Phase S population was very few after 0.5mM ACR treated BMMSCs for 72 h. Differences between the control and treated cells were not statistically significant (P<0.05). The cell cycle was analyzed by flow cytometry after propidium iodide (PI) staining, and data were processed with the ModFit LT program.
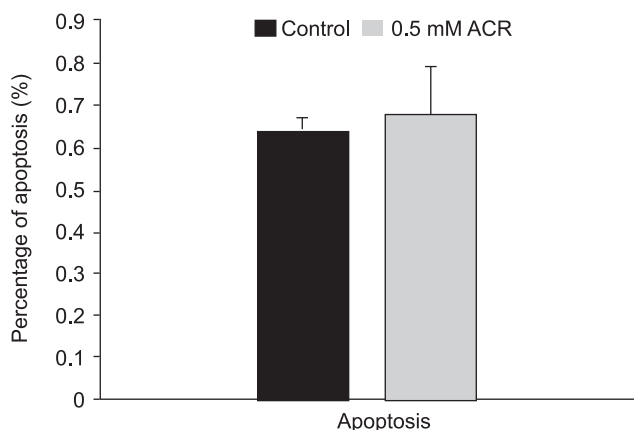

Fig. 6. Increased apoptosis in bMMSCs after 0.5mM ACR induced for 72 h, assessed by flow cytometry analysis of the annexin V staining. The percentage was N(Apoptosis) /N (Total cells). There was no statistically significant difference between the control and treated cells (P<0.05).

Hogervorst J G, Schouten L J, Konings E J, Goldbohm R A and van den Brandt P A. 2007. A prospective study of dietary acrylamide intake and the risk of endometrial, ovarian, and breast cancer. *Cancer Epidemiology, Biomarkers and Prevention* **16**: 2304–13.

Hogervorst J G, Schouten L J, Konings E J, Goldbohm R A and Van den Brandt P A. 2008. Dietary acrylamide intake and the risk of renal cell, bladder, and prostate cancer. *American Journal of Clinical Nutrition* **87**: 1428–38.

Huang L, Niu C, Willard B, Zhao W, Liu L, He W, Wu T, Yang S, Feng S, Mu Y, Zheng L and Li K. 2015. Proteomic analysis of porcine mesenchymal stem cells derived from bone marrow and umbilical cord: implication of the proteins involved in the higher migration capability of bone marrow mesenchymal stem cells. *Stem Cell Research and Therapy* **6**: 77.

Imai Y, Kuba K, Neely G G, Yaghubian-Malhami R, Perkmann T, Van Loo G, Ermolaeva M, Veldhuizen R, Leung Y H, Wang H, Liu H, Sun Y, Pasparakis M, Kopf M, Mech C, Bavari S, Peiris J S, Slutsky A S, Akira S, Hultqvist M, Holmdahl R, Nicholls J, Jiang C, Binder C J and Penninger J M. 2008. Identification of oxidative stress and Toll-like receptor 4 signaling as a key pathway of acute lung injury. *Cell* **133**: 235–49.

Keating A. 2006. Mesenchymal stromal cells. *Current Opinion in Hematology* **13**: 419–25.

Konings E J, Ashby P, Hamlet C G and Thompson G A. 2007. Acrylamide in cereal and cereal products: a review on progress in level reduction. *Food Additives & Contaminants* 24 Suppl **1**: 47–59.

Li H, Ma G, Gui D, Zhao S, Wang P, He K, Wang X, Ruan J, Cao J and Yang S. 2011. Characterization of the porcine p65 subunit of NF-[kappa] B and its association with virus antibody levels. *Molecular Immunology* **48** (6–7): 914–23.

Markovina S, Callander N S, O'Connor S L, Xu G, Shi Y, Leith C P, Kim K, Trivedi P, Kim J, Hematti P and Miyamoto S.2010. Bone marrow stromal cells from multiple myeloma patients uniquely induce bortezomib resistant NF-kappaB activity in myeloma cells. *Molecular Cancer* **9**: 176.

Pelucchi C, Bosetti C, Galeone C and La Vecchia C. 2015. Dietary acrylamide and cancer risk: an updated meta-analysis. *International Journal of Cancer* **136**: 2912–22.

Pennisi M, Malaguarnera G, Puglisi V, Vinciguerra L, Vacante M and Malaguarnera M. 2013. Neurotoxicity of acrylamide in exposed workers. *International Journal of Environmental Research and Public Health* **10**: 3843–54.

Tanaka Y. 2015. Human mesenchymal stem cells as a tool for joint repair in rheumatoid arthritis. *Clinical and Experimental Rheumatology* **33**: S58–62.

Trivedi P and Hematti P. 2008. Derivation and immunological characterization of mesenchymal stromal cells from human embryonic stem cells. *Experimental Hematology* **36**: 350–59.

Vinoth K J, Manikandan J, Sethu S, Balakrishnan L, Heng A, Lu K, Poonepalli A, Hande M P and Cao T. 2015. Differential resistance of human embryonic stem cells and somatic cell types to hydrogen peroxide-induced genotoxicity may be dependent on innate basal intracellular ROS levels. *Folia Histochemica et Cytobiologica* **53**: 169–74.